

Figure 1: Computed (dots) density and internal energy for Test # 1 using Godunov-MUSCL scheme, compared with exact solution (solid line) at $t=0.035$; $\Delta\xi = 0.01$. Unified coordinates, $h = 0$ (Eulerian).

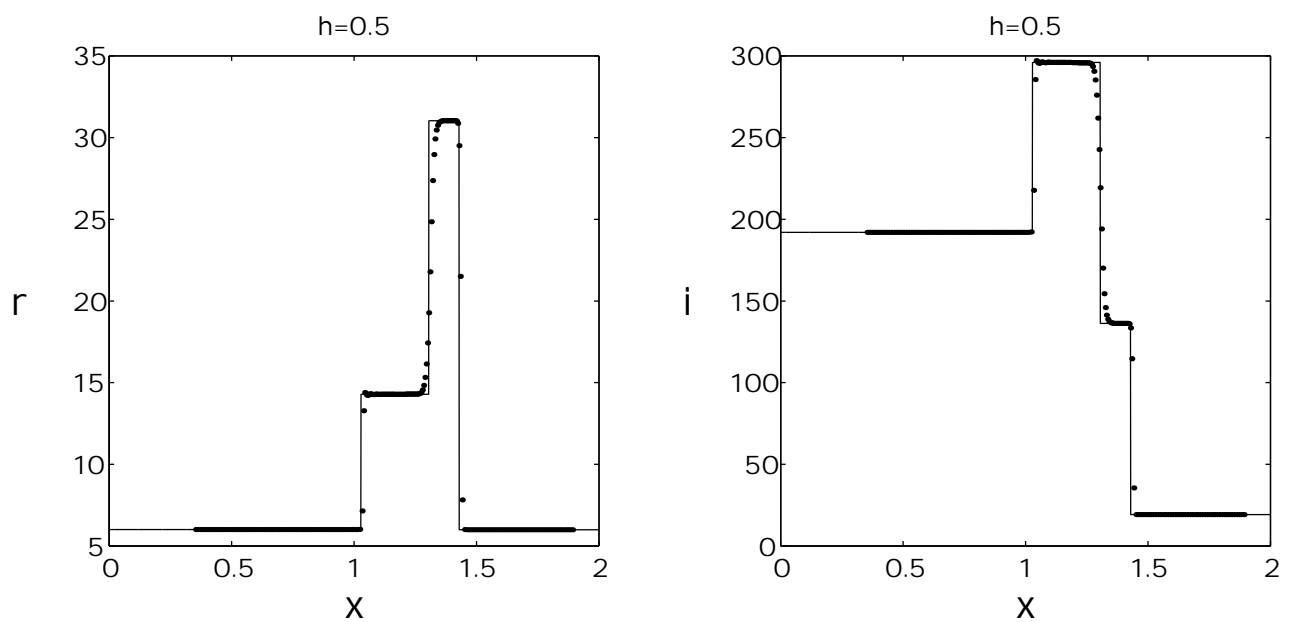


Figure 2: Computed (dots) density and internal energy for Test # 1 using Godunov-MUSCL scheme, compared with exact solution (solid line) at $t=0.035$; $\Delta\xi = 0.01$. Unified coordinates , $h = 0.5$.

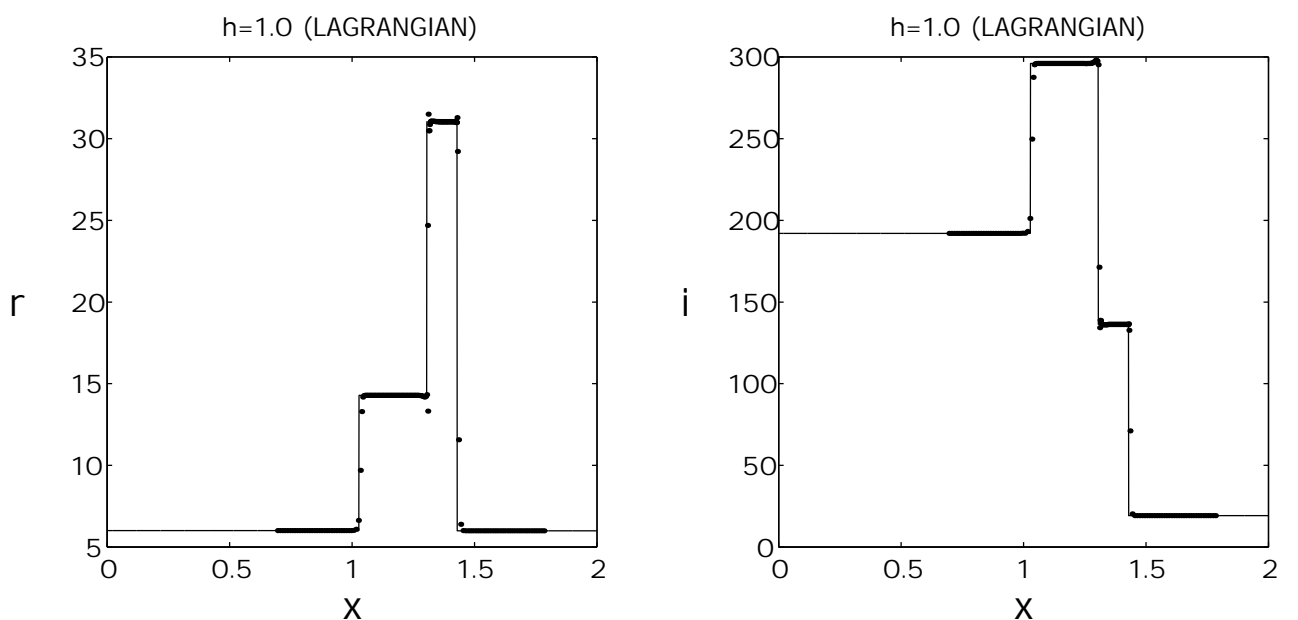


Figure 3: Computed (dots) density and internal energy for Test # 1 using Godunov-MUSCL scheme, compared with exact solution (solid line) at $t=0.035$; $\Delta\xi = 0.01$. Unified coordinates, $h = 1$ (Lagrangian).

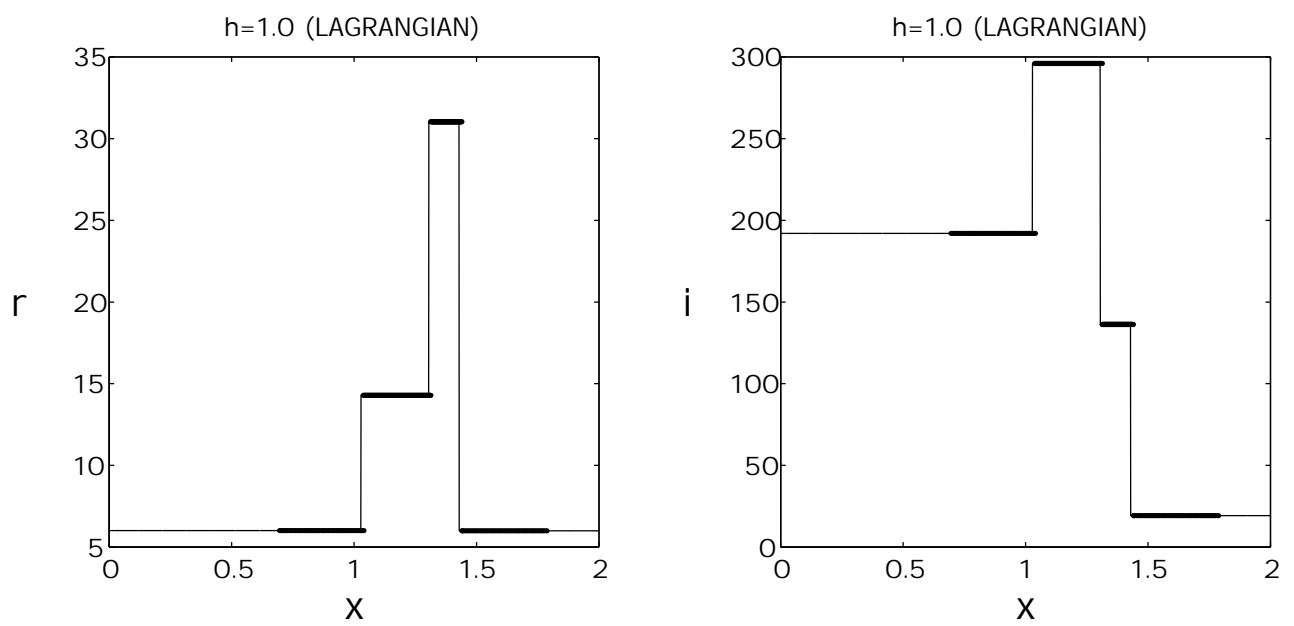


Figure 4: Computed (dots) density and internal energy for Test # 1 using shock-adaptive Godunov scheme, compared with exact solution (solid line) at $t=0.035$; $\Delta\xi = 0.01$. Unified coordinates, $h = 1$ (Lagrangian).

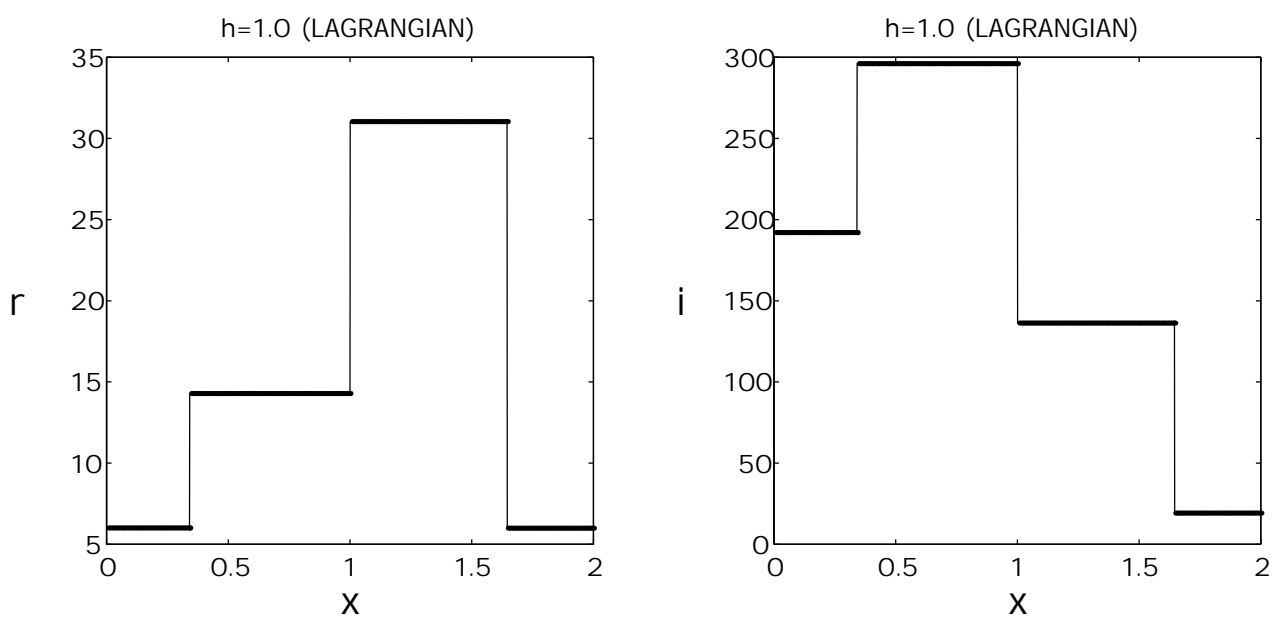


Figure 5: Computed (dots) density and internal energy as function of ξ for Test # 1 using shock-adaptive Godunov scheme, compared with exact solution (solid line) at $t=0.035$; $\Delta\xi = 0.01$. Unified coordinates, $h = 1$ (Lagrangian).

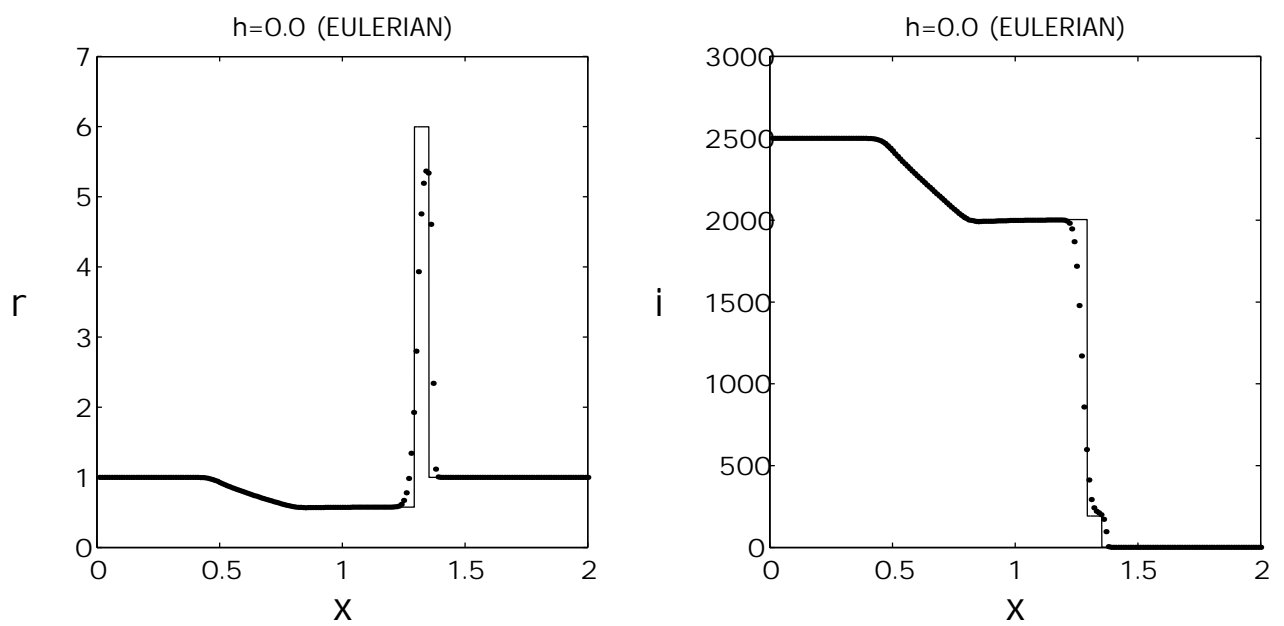


Figure 6: Computed (dots) density and internal energy for Test # 2 using Godunov-MUSCL scheme, compared with exact solution (solid line) at $t=0.015$; $\Delta x = 0.01$. Unified coordinates, $h = 0$ (Eulerian).

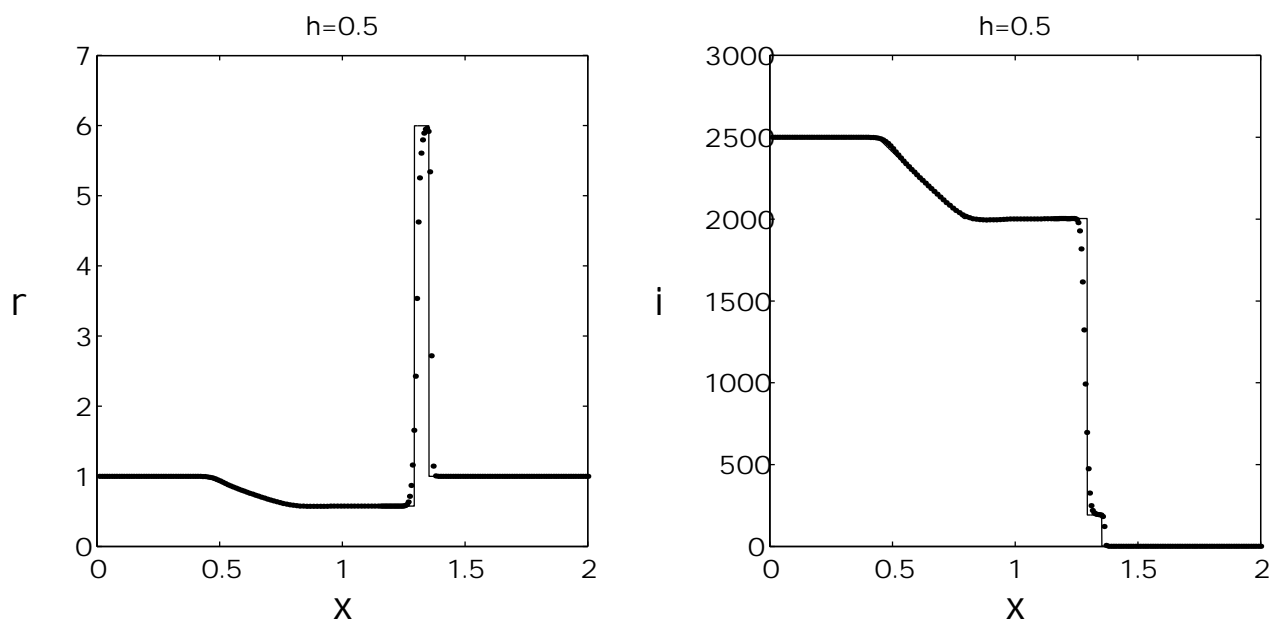


Figure 7: Computed (dots) density and internal energy for Test # 2 using Godunov-MUSCL scheme, compared with exact solution (solid line) at $t=0.015$; $\Delta\xi = 0.01$. Unified coordinates , $h = 0.5$.

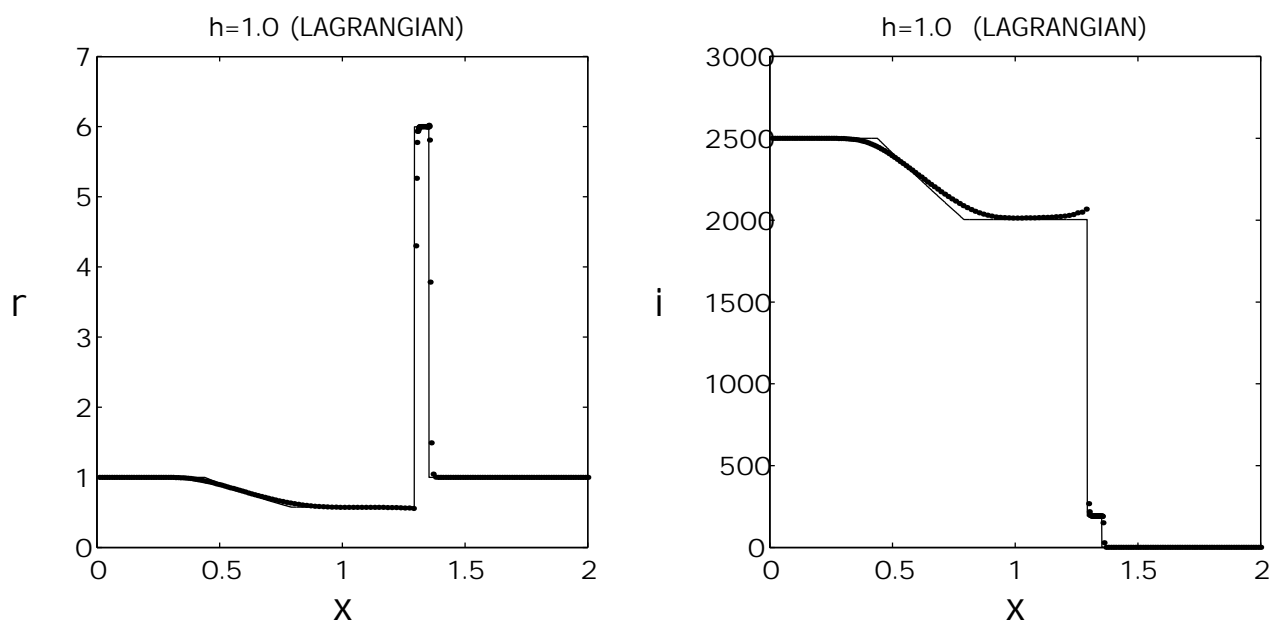


Figure 8: Computed (dots) density and internal energy for Test # 2 using Godunov-MUSCL scheme, compared with exact solution (solid line) at $t=0.015$; $\Delta\xi = 0.01$. Unified coordinates, $h = 1$ (Lagrangian).

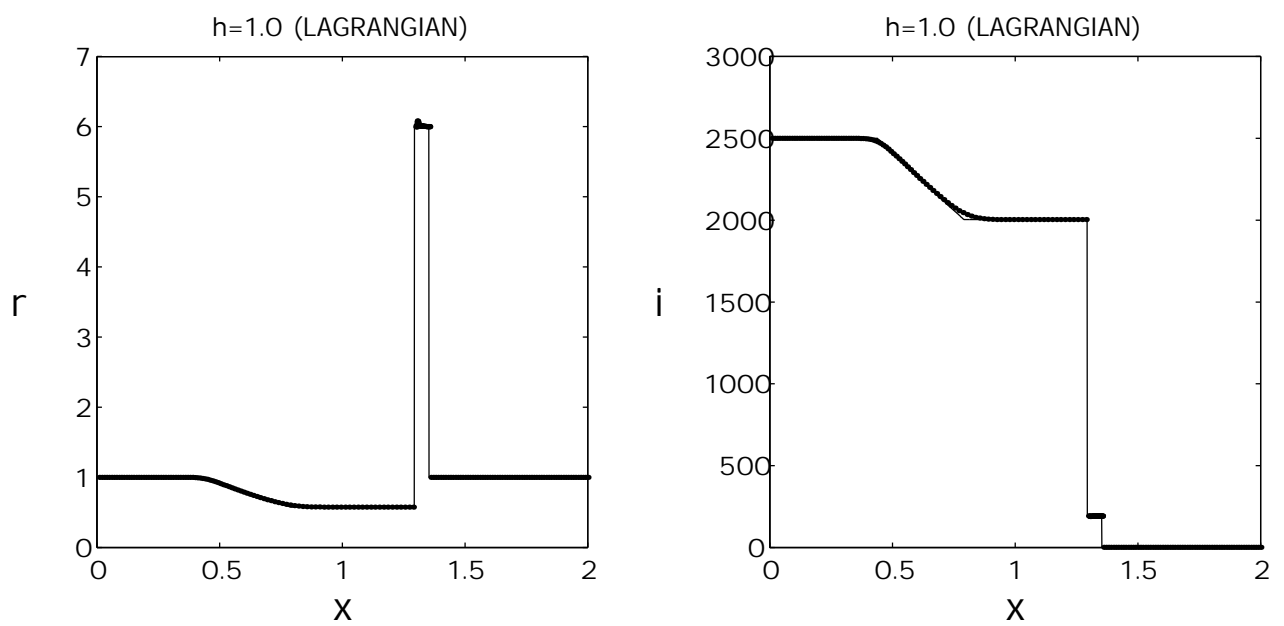


Figure 9: Computed (dots) density and internal energy for Test # 2 using shock-adaptive Godunov scheme, compared with exact solution (solid line) at $t=0.015$; $\Delta\xi = 0.01$. Unified coordinates, $h = 1$ (Lagrangian).

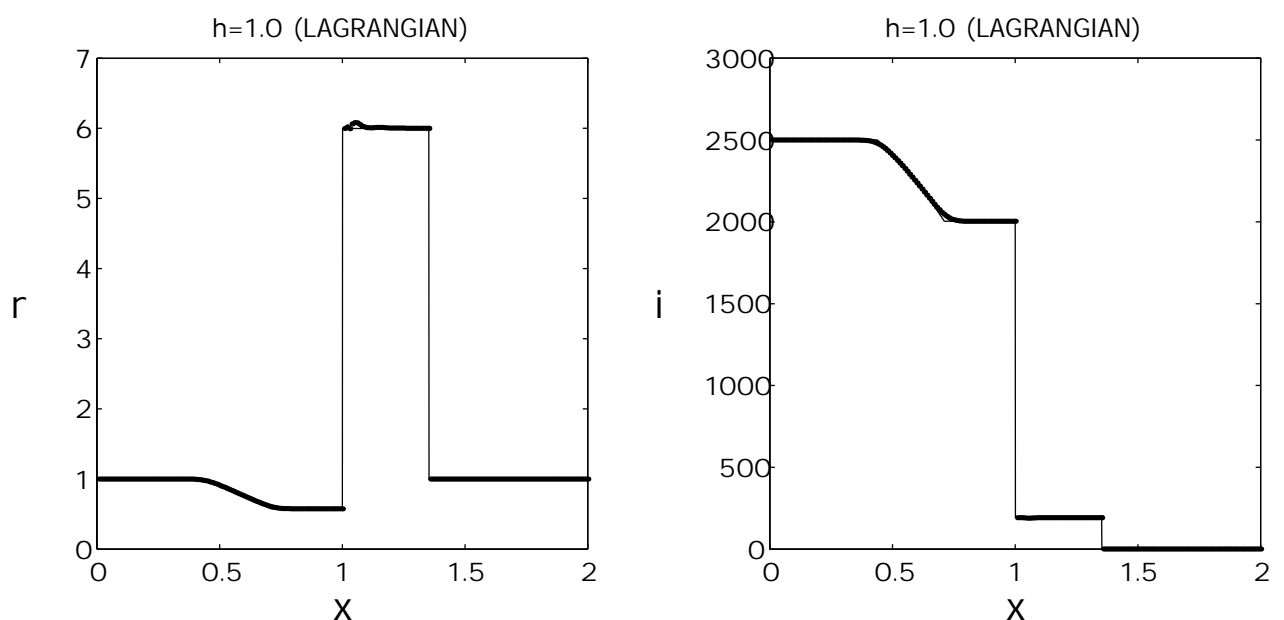


Figure 10: Computed (dots) density and internal energy as function of ξ for Test # 2 using shock-adaptive Godunov scheme, compared with exact solution (solid line) at $t=0.015$; $\Delta\xi = 0.01$. Unified coordinates, $h = 1$ (Lagrangian).

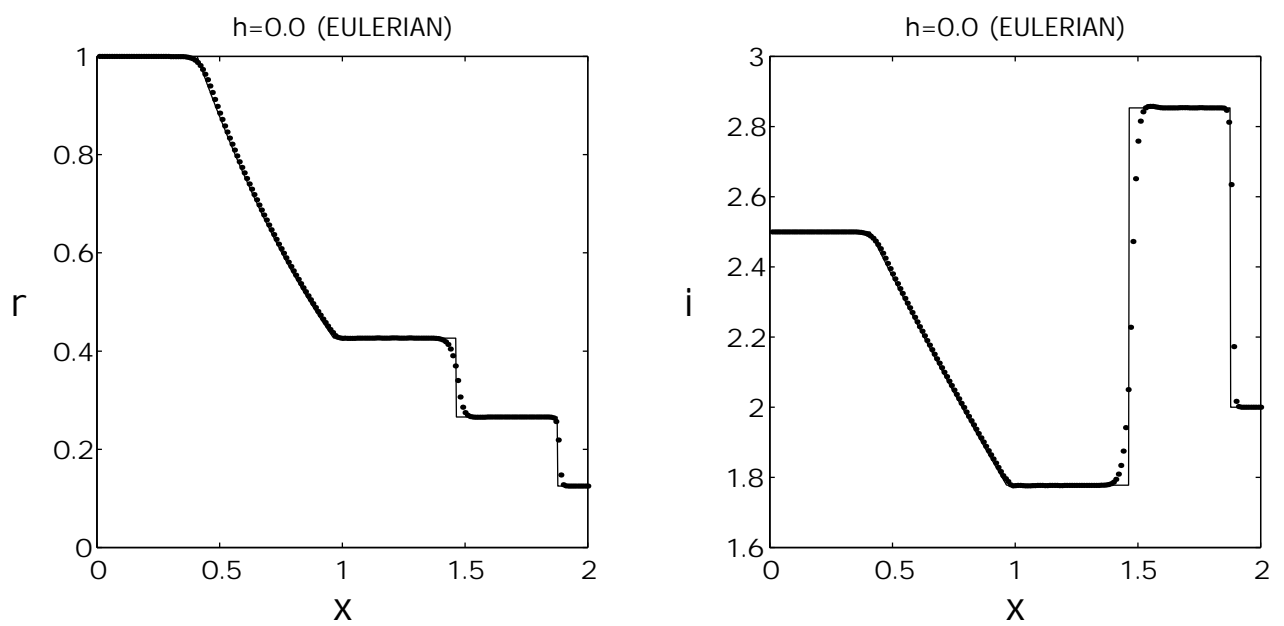


Figure 11: Computed (dots) density and internal energy for Test # 3 using Godunov-MUSCL scheme, compared with exact solution (solid line) at $t=0.5$; $\Delta x = 0.01$. Unified coordinates, $h = 0$ (Eulerian).

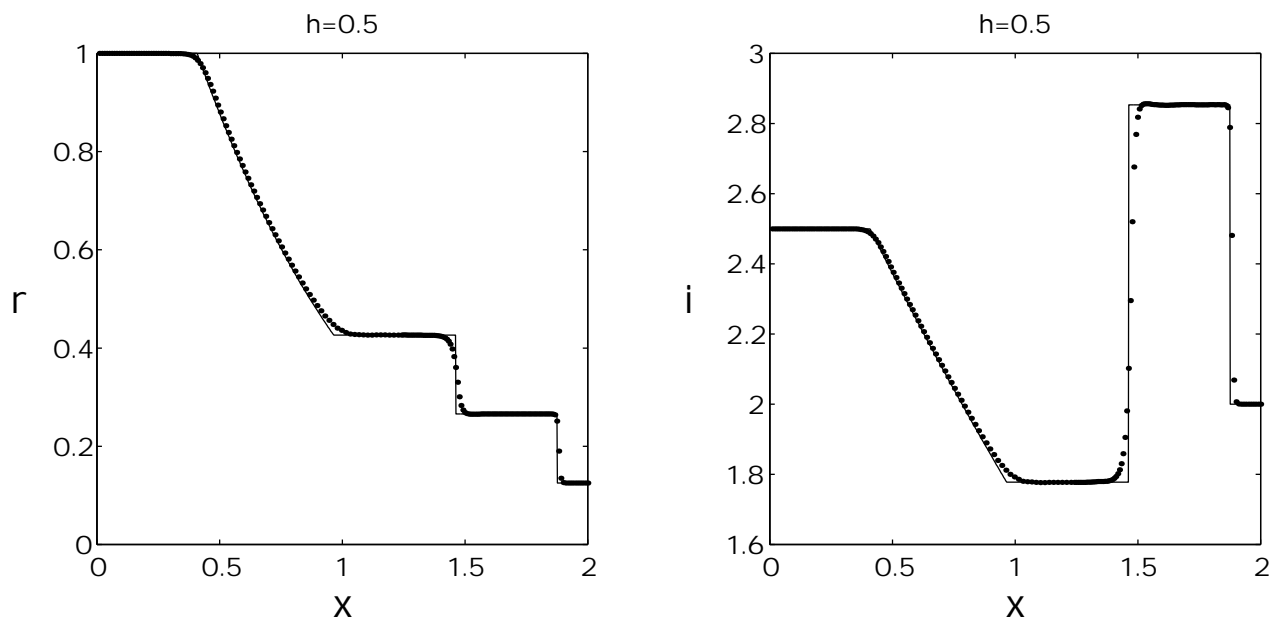


Figure 12: Computed (dots) density and internal energy for Test # 3 using Godunov-MUSCL scheme, compared with exact solution (solid line) at $t=0.5$; $\Delta\xi = 0.01$. Unified coordinates , $h = 0.5$.

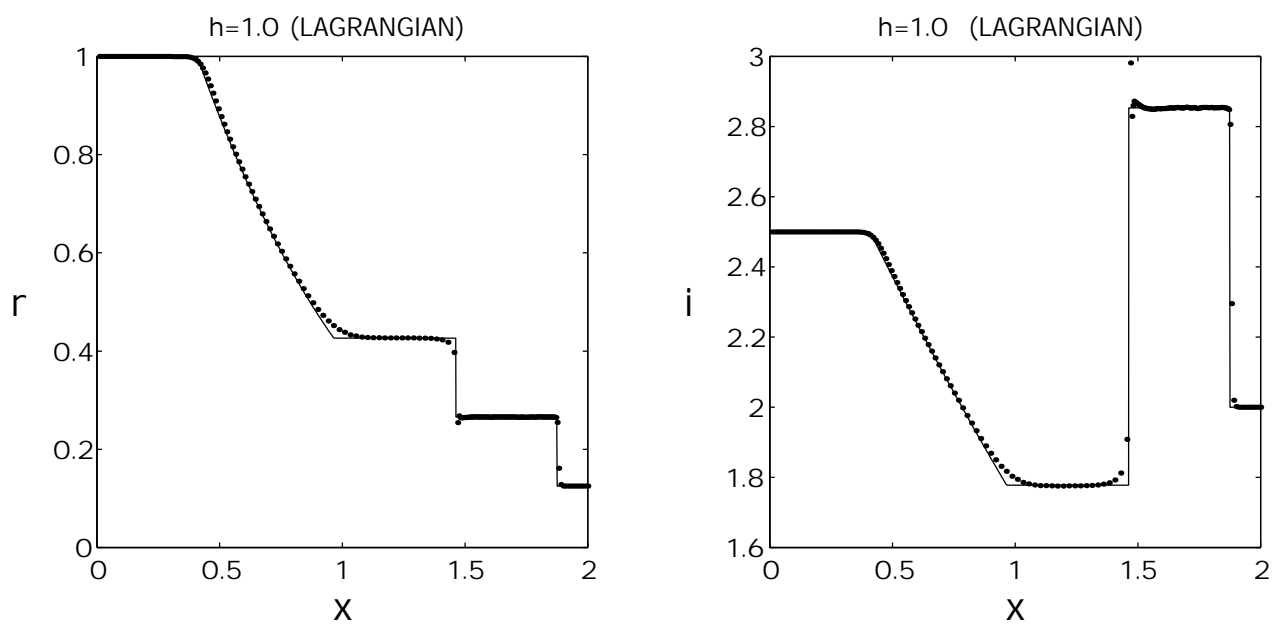


Figure 13: Computed (dots) density and internal energy for Test # 3 using Godunov-MUSCL scheme, compared with exact solution (solid line) at $t=0.5$; $\Delta\xi = 0.01$. Unified coordinates, $h = 1$ (Lagrangian).

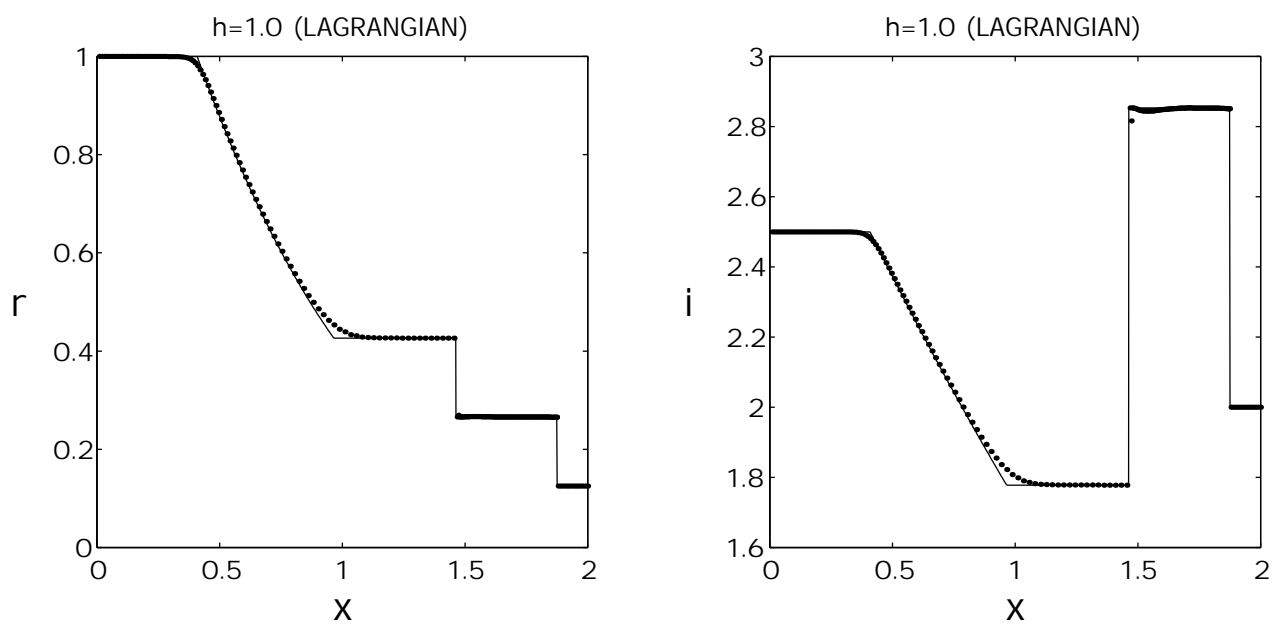


Figure 14: Computed (dots) density and internal energy for Test # 3 using shock-adaptive Godunov scheme, compared with exact solution (solid line) at $t=0.5$; $\Delta\xi = 0.01$. Unified coordinates, $h = 1$ (Lagrangian).

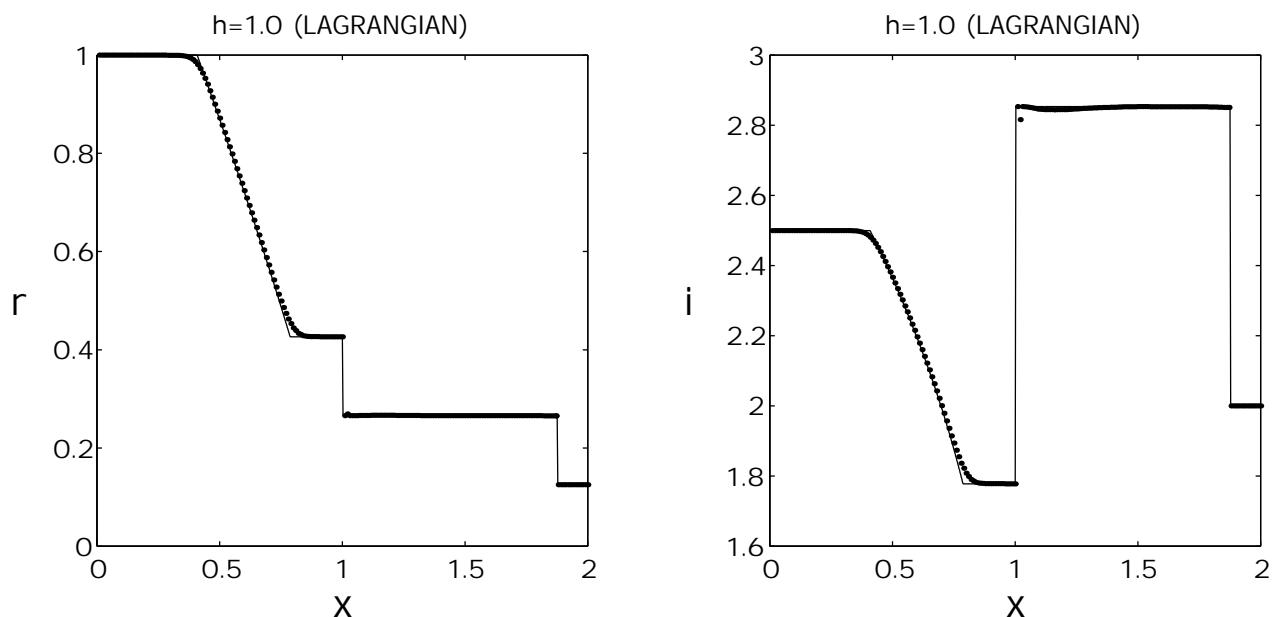


Figure 15: Computed (dots) density and internal energy as function of ξ for Test # 3 using shock-adaptive Godunov scheme, compared with exact solution (solid line) at $t=0.5$; $\Delta\xi = 0.01$. Unified coordinates, $h = 1$ (Lagrangian).

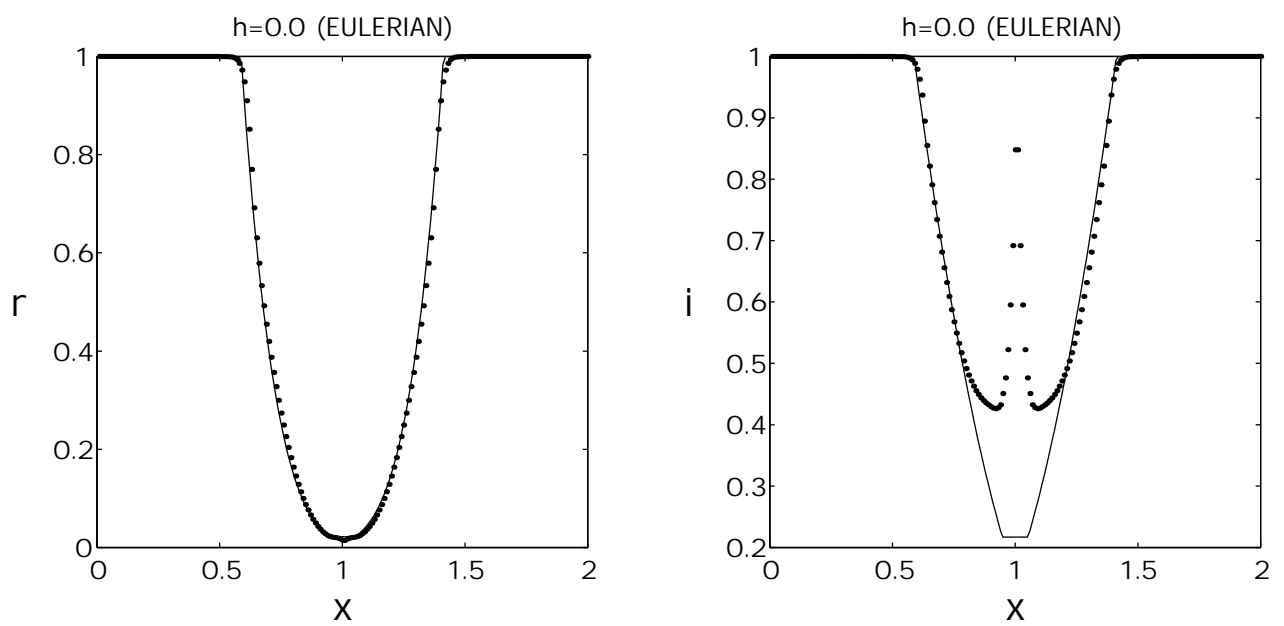


Figure 16: Computed (dots) density and internal energy for Test # 4 using Godunov-MUSCL scheme, compared with exact solution (solid line) at $t=0.15$; $\Delta x = 0.01$. Unified coordinates, $h = 0$ (Eulerian).

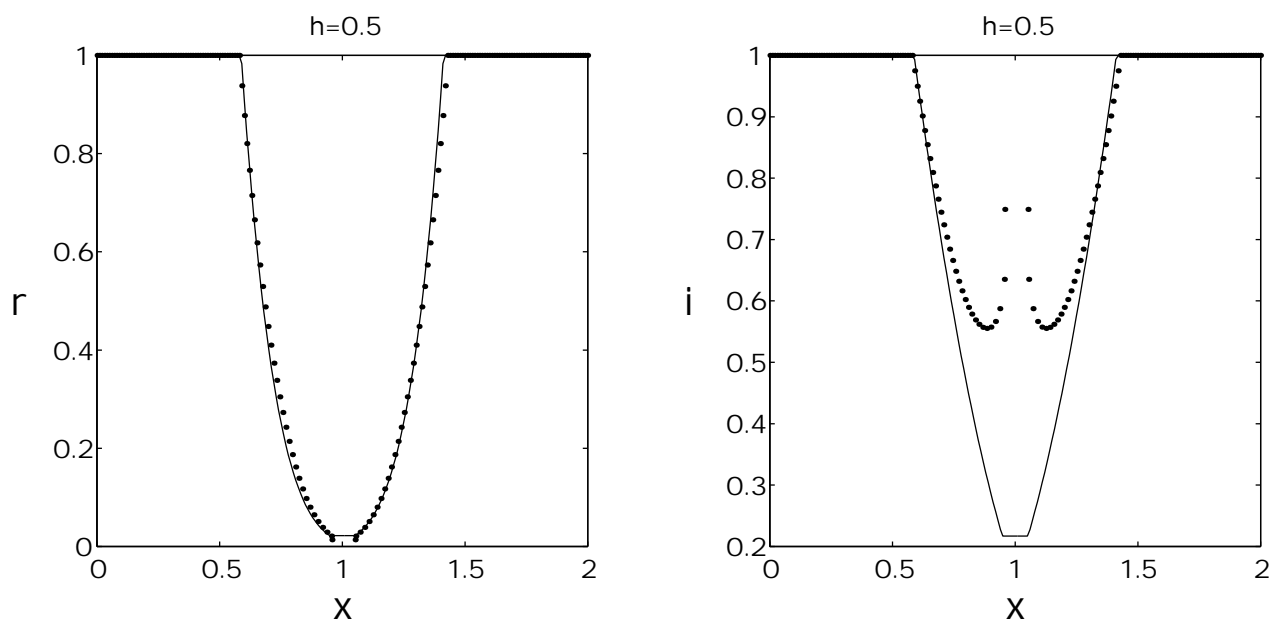


Figure 17: Computed (dots) density and internal energy for Test # 4 using Godunov-MUSCL scheme, compared with exact solution (solid line) at $t=0.15$; $\Delta\xi = 0.01$. Unified coordinates , $h = 0.5$.

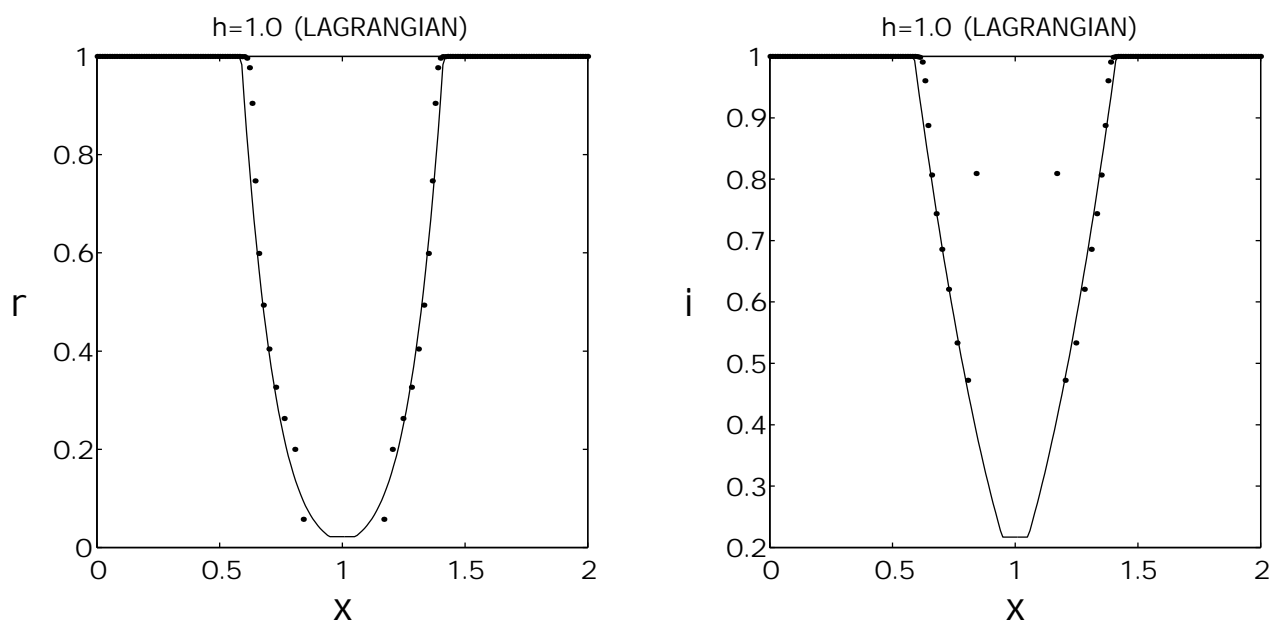


Figure 18: Computed (dots) density and internal energy for Test # 4 using Godunov-MUSCL scheme, compared with exact solution (solid line) at $t=0.15$; $\Delta\xi = 0.01$. Unified coordinates, $h = 1$ (Lagrangian).

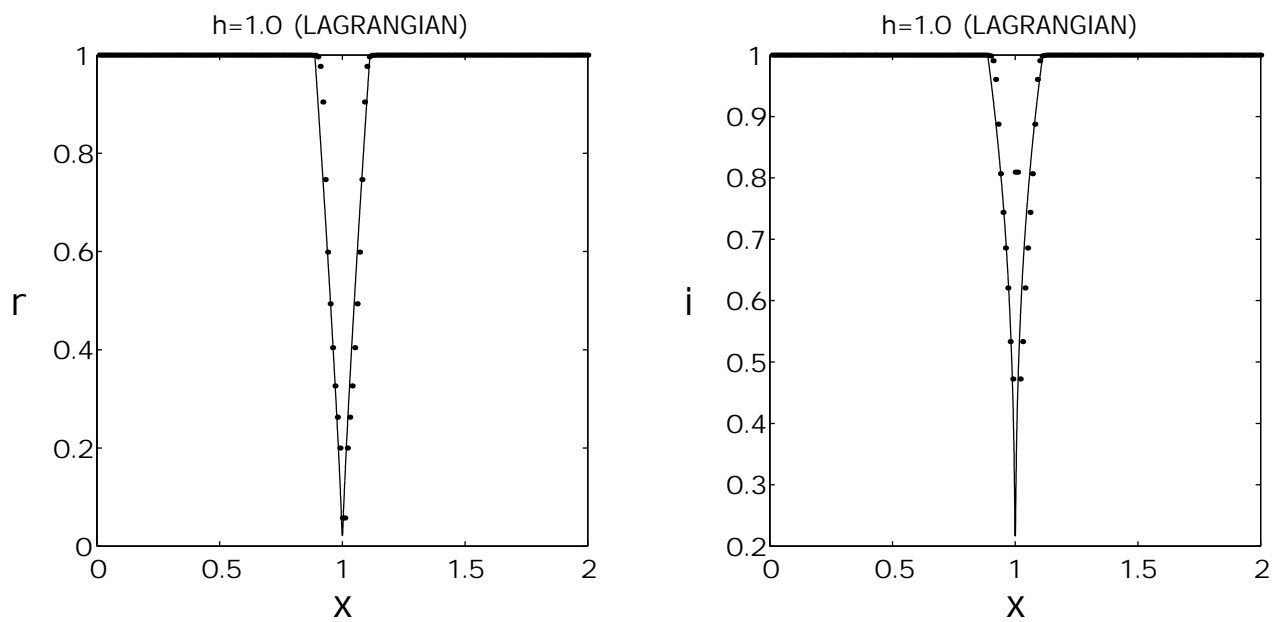


Figure 19: Computed (dots) density and internal energy as function of ξ for Test # 4 using Godunov-MUSCL scheme, compared with exact solution (solid line) at $t=0.15$; $\Delta\xi = 0.01$. Unified coordinates, $h = 1$ (Lagrangian).

Figure 20: Test # 5. Results from A.Harten and J.M Hyman [20] computed at $t=0.15$; $\Delta x = 0.01$.

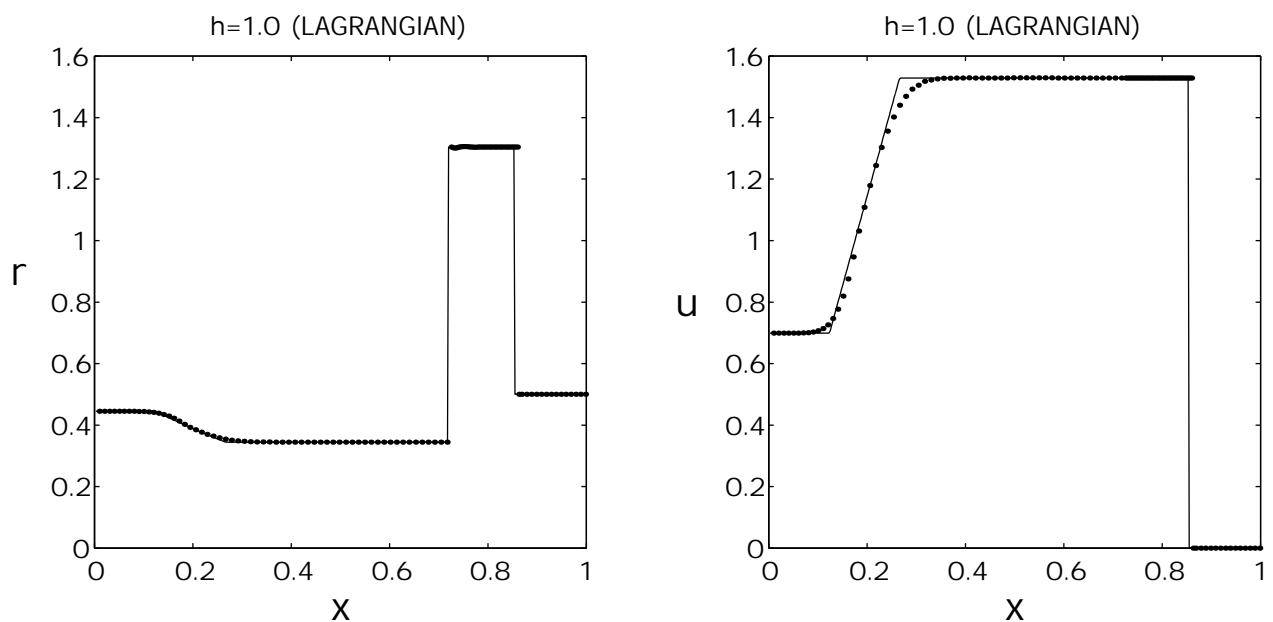


Figure 21: Computed (dots) density and velocity for Test # 5 using shock-adaptive Godunov scheme, compared with exact solution (solid line) at $t=0.15$; $\Delta \xi = 0.01$. Unified coordinates, $h = 1$ (Lagrangian).

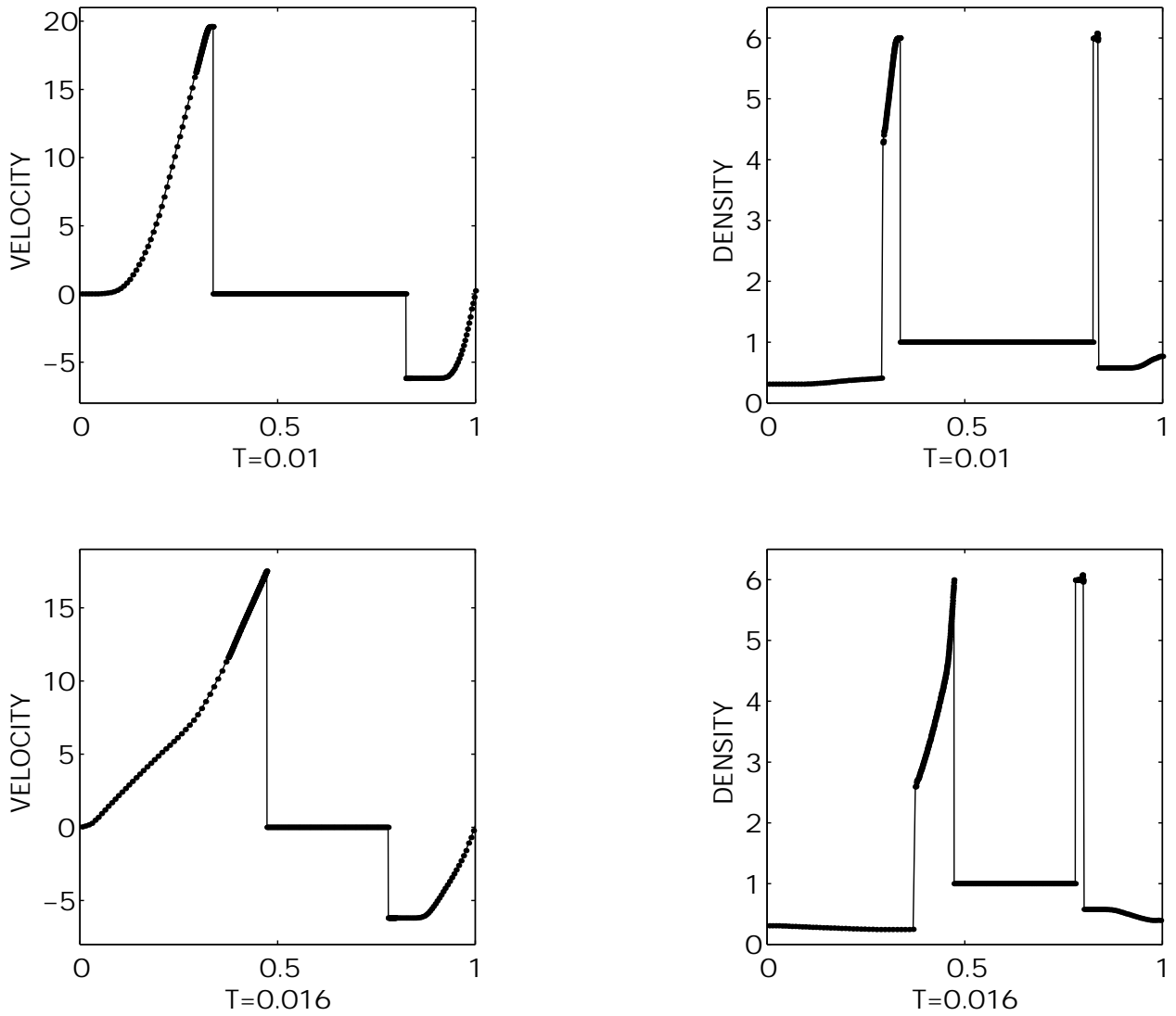
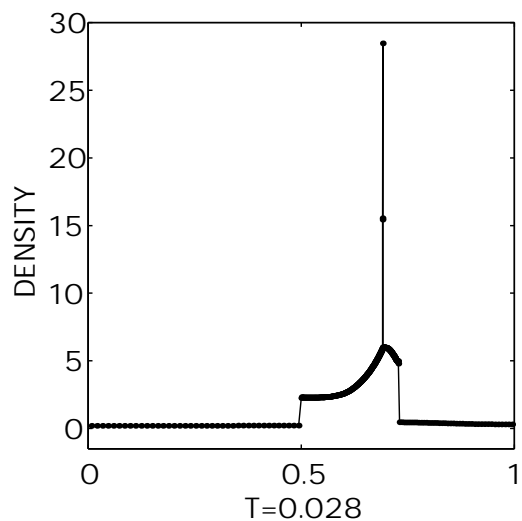
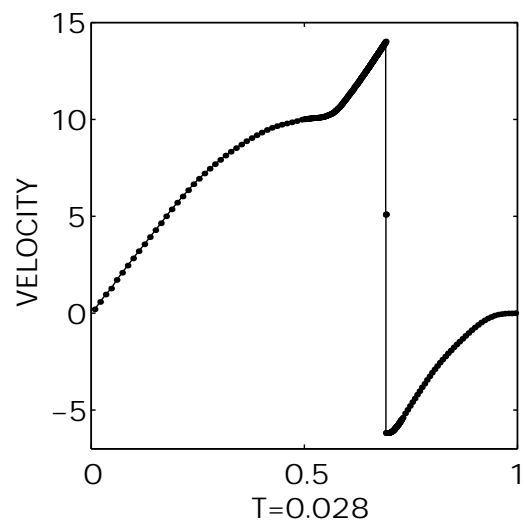
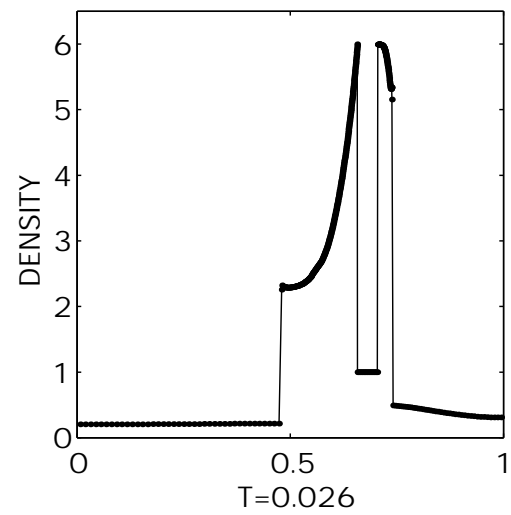
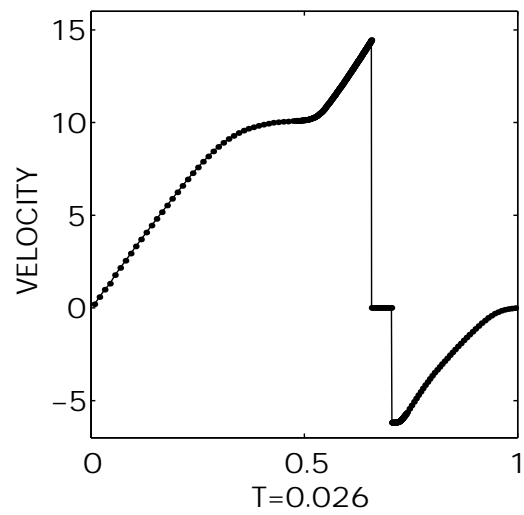


Figure 22: Computed density and velocity at different times for the "Bang-bang" problem of Woodward and Colella [24] using shock-adaptive Godunov scheme; $\Delta\xi = 0.0025$. Unified coordinates, $h = 1$ (Lagrangian).



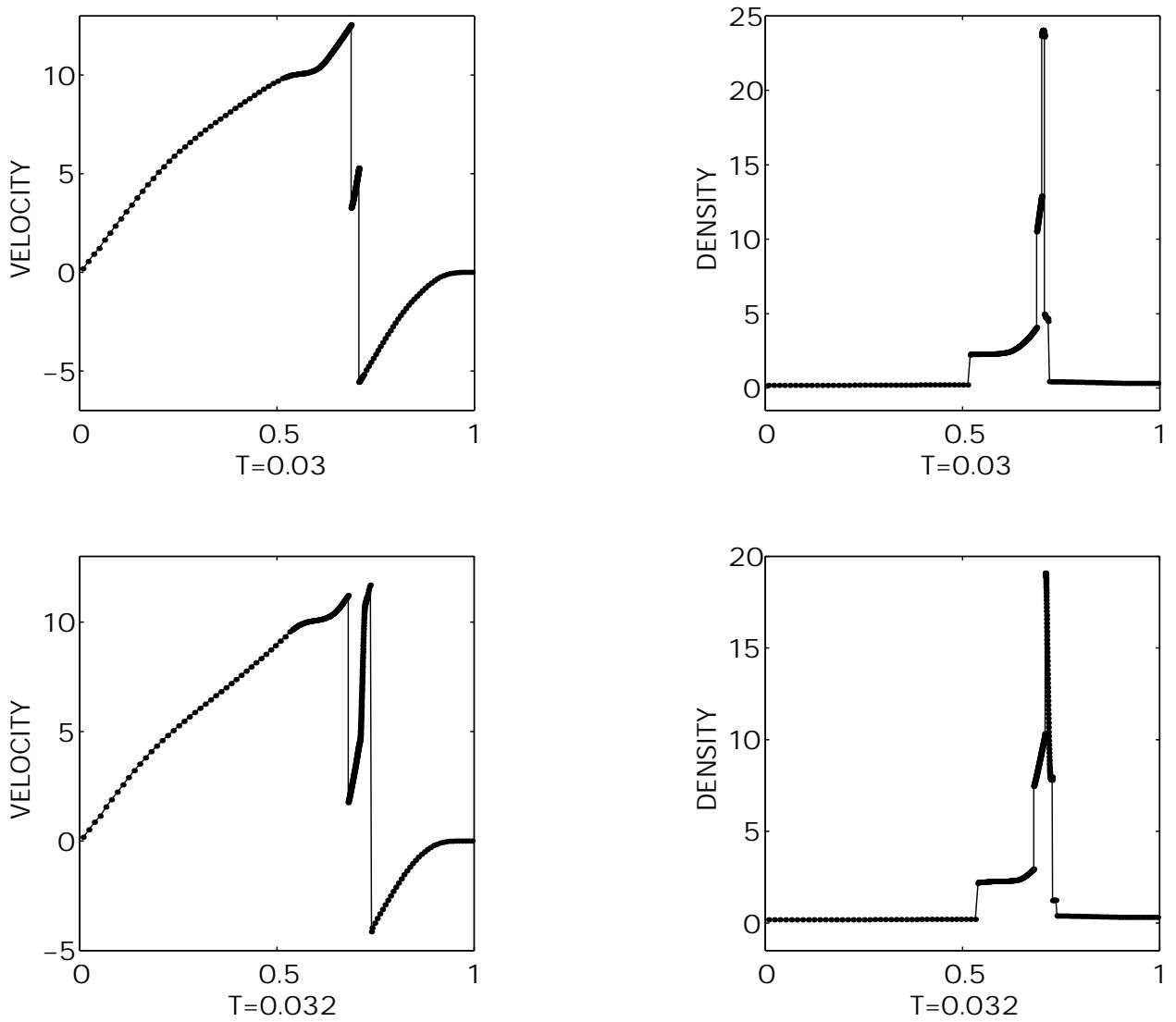
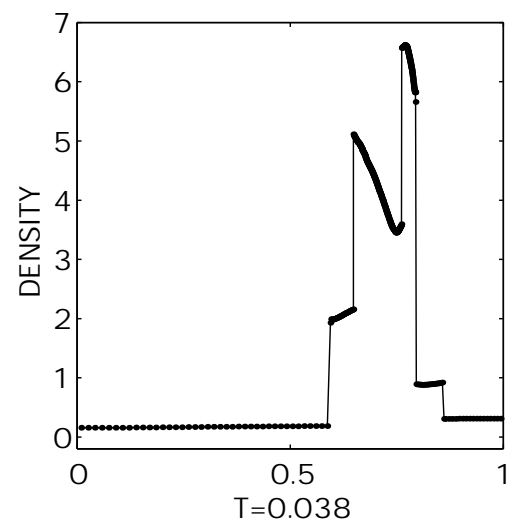
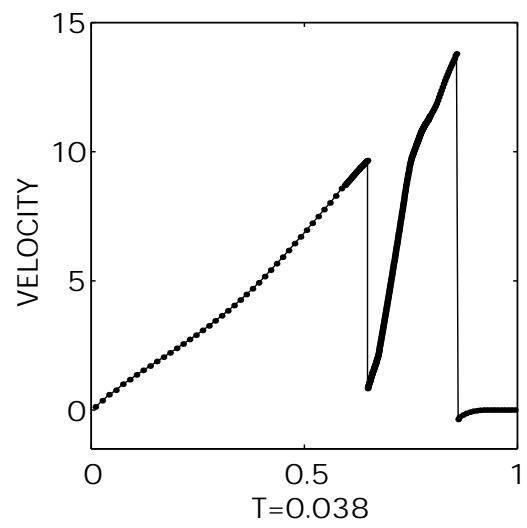
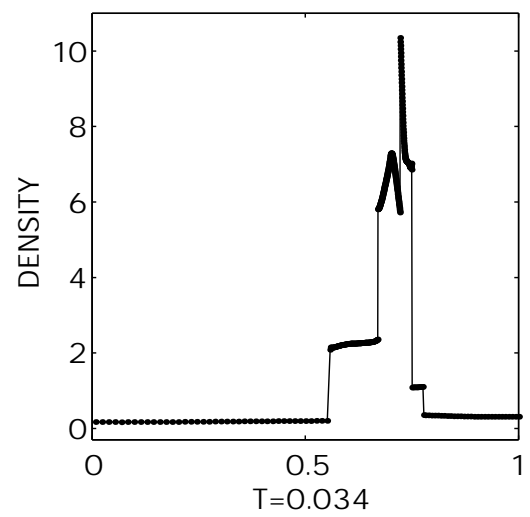
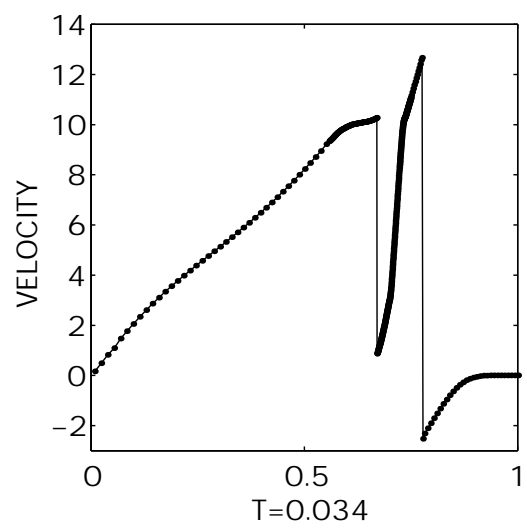


Figure 23: Computed density and velocity at different times for the "Bang-bang" problem of Woodward and Colella [24] using shock-adaptive Godunov scheme; $\Delta\xi = 0.0025$. Unified coordinates, $h = 1$ (Lagrangian).



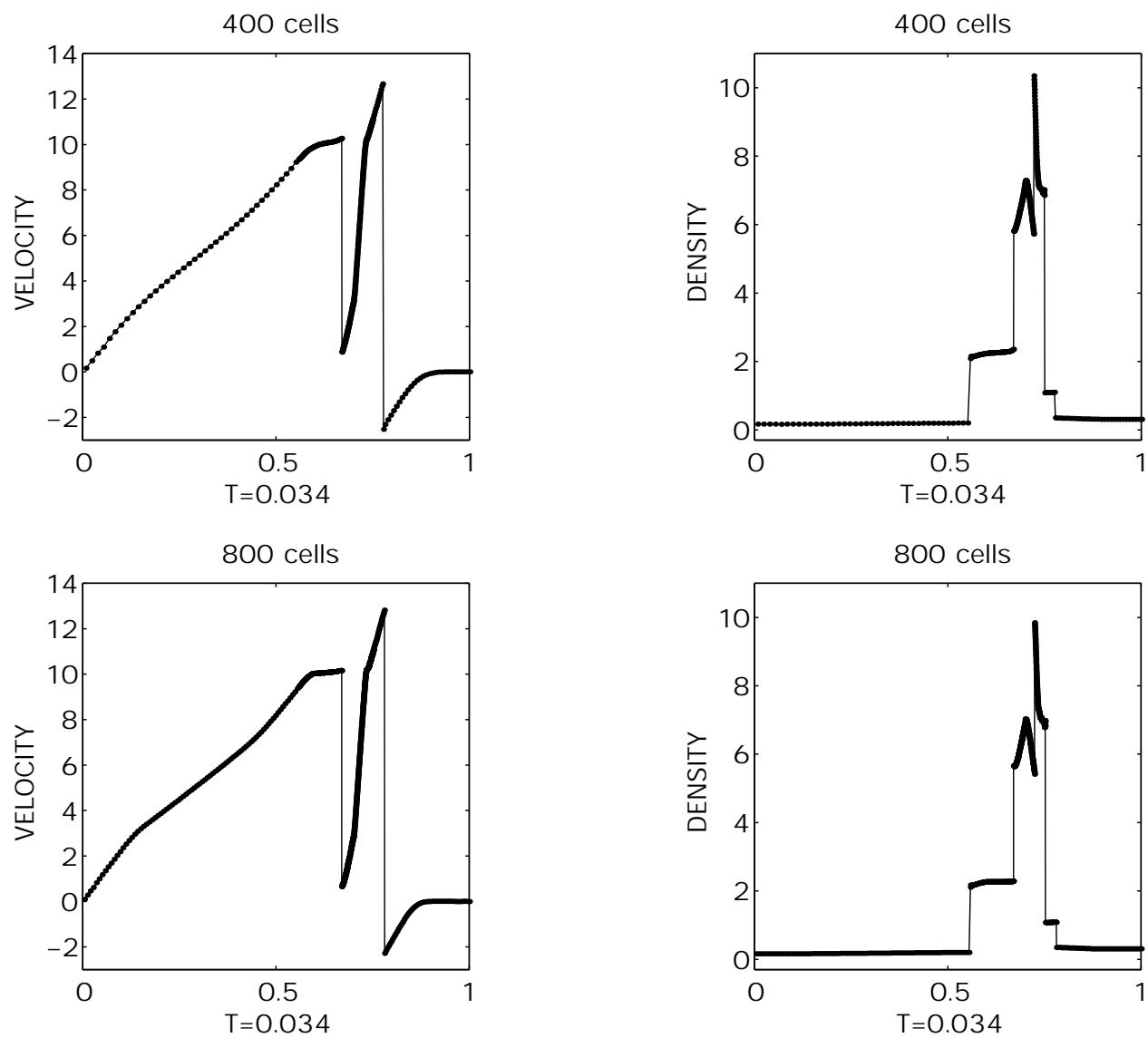


Figure 24: Comparison of present computed results using 400 and 800 cells in the "Bang-bang" problem of Woodward and Colella [24]

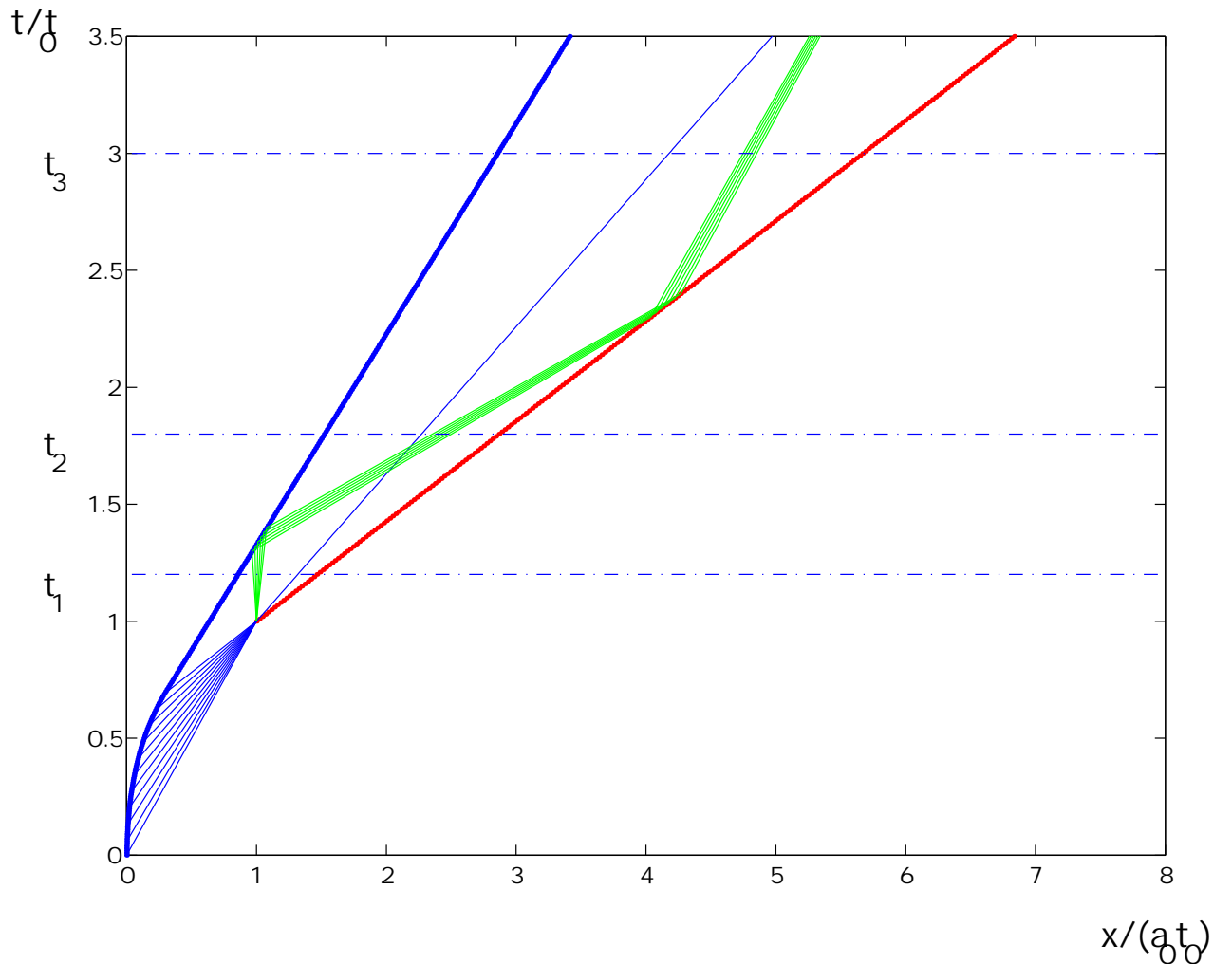


Figure 25: Sketch of waves in the problem of sudden formation of shock wave inside a shock tube; the piston path is given by $x(t) = \frac{\gamma+1}{\gamma-1} a_0 t_0 \left(1 - \frac{2t}{(\gamma+1)t_0} - \left(1 - \frac{t}{t_0}\right)^{\frac{2}{\gamma+1}} \right)$.

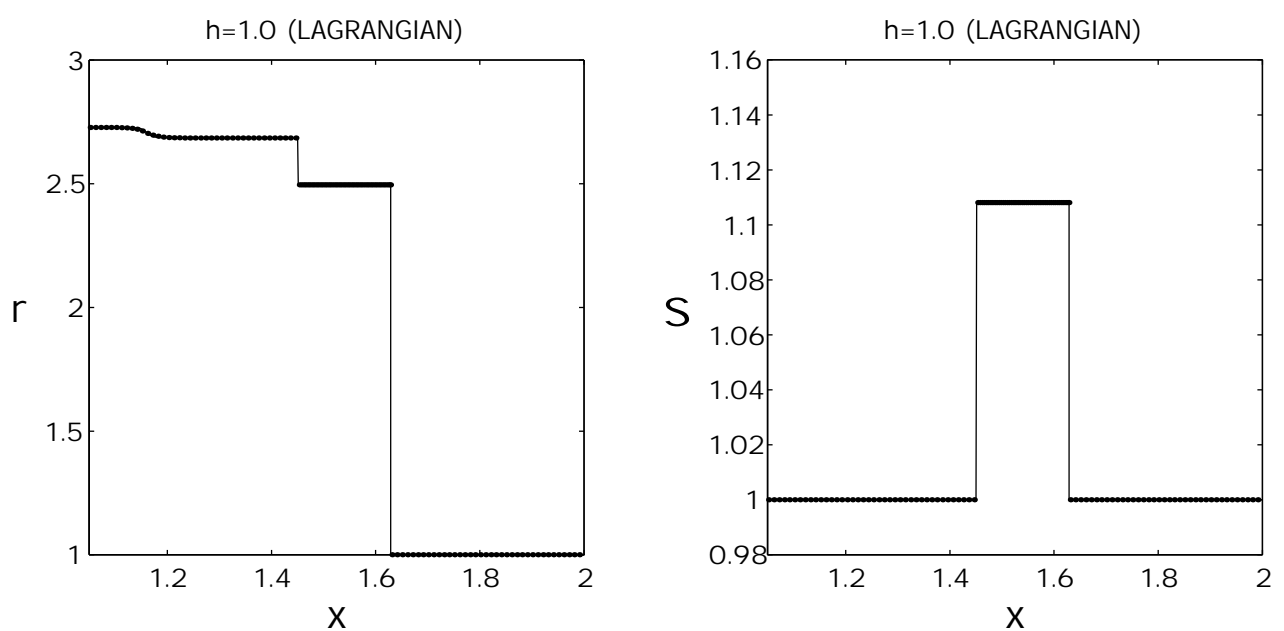


Figure 26: Piston Problem. Comparison of solution with $\Delta\xi = 0.01$ (dotted line) with solution with $\Delta\xi = 0.001$ (solid line) at $t=1.2$

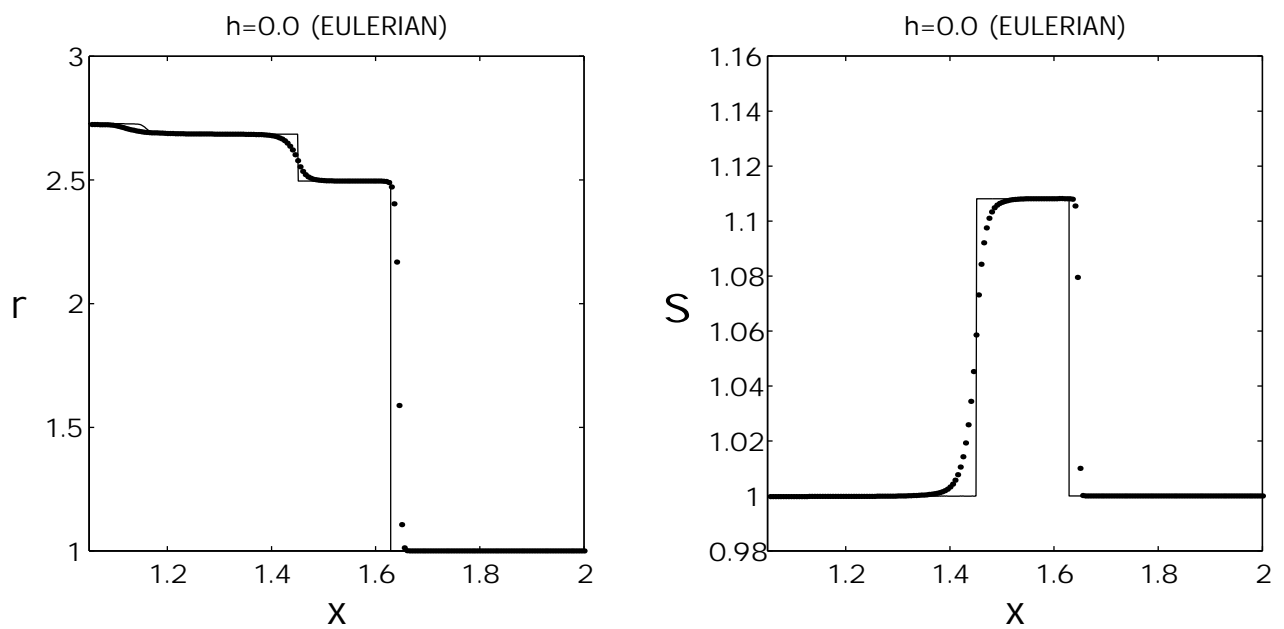


Figure 27: Computed (dots) density and entropy for the piston problem using Godunov-MUSCL scheme, compared with exact solution (solid line) at $t_1 = 1.2$; $\Delta x = 0.005$. Unified coordinates, $h = 0$ (Eulerian).

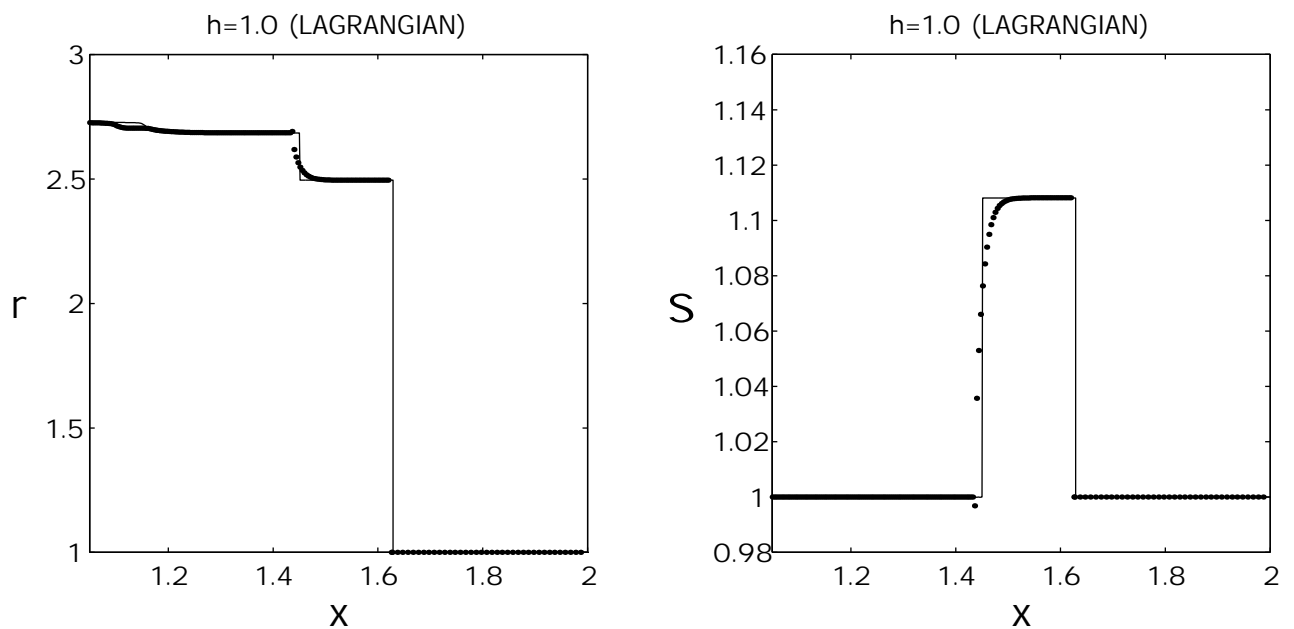


Figure 28: Computed (dots) density and entropy for the piston problem using shock-adaptive Godunov scheme, compared with exact solution (solid line) at $t_1 = 1.2$; $\Delta x = 0.01$. Unified coordinates, $h = 1$ (Lagrangian).

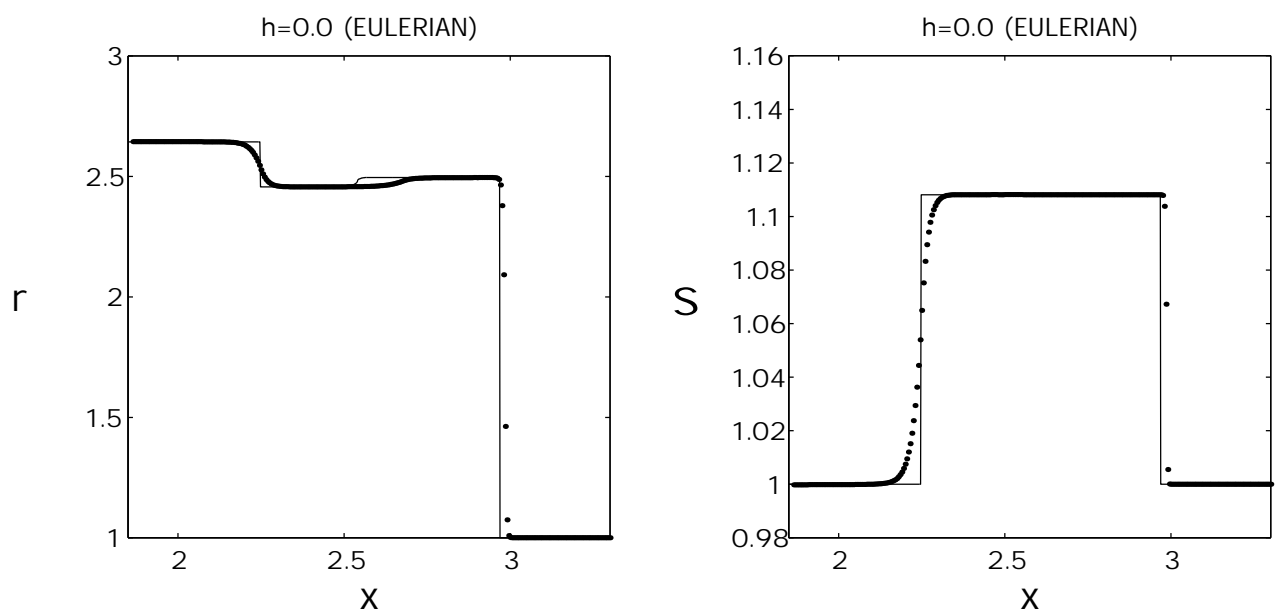


Figure 29: Computed (dots) density and entropy for the piston problem using Godunov-MUSCL scheme, compared with exact solution (solid line) at $t_2 = 1.8$; $\Delta x = 0.005$. Unified coordinates, $h = 0$ (Eulerian).

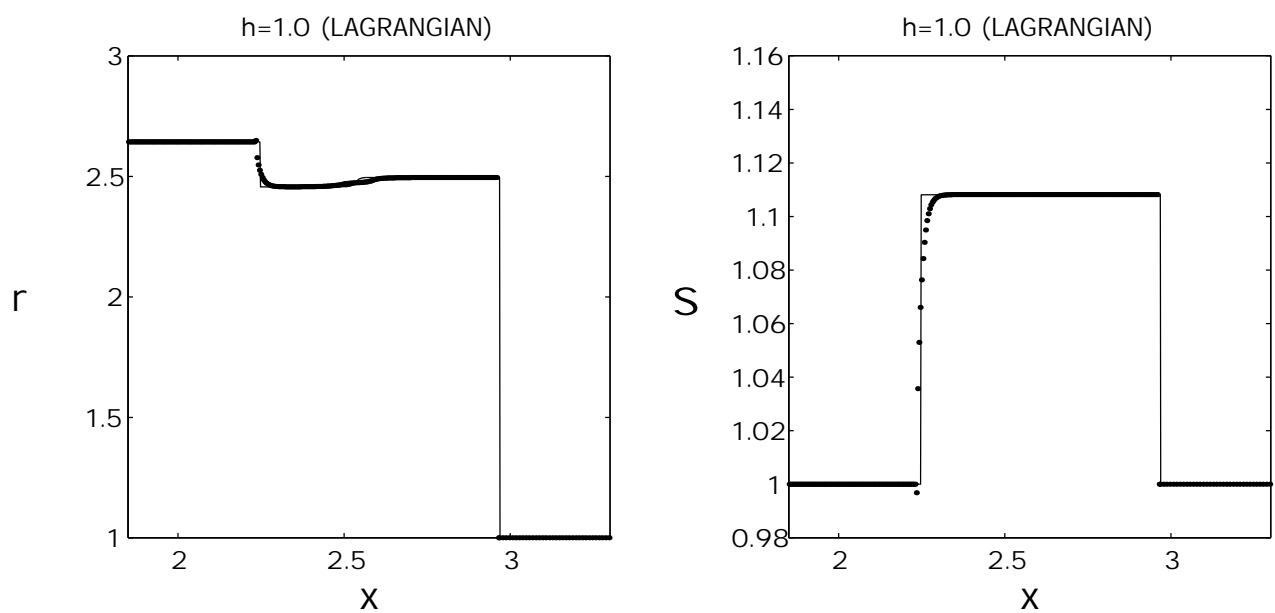


Figure 30: Computed (dots) density and entropy for the piston problem using shock-adaptive Godunov scheme, compared with exact solution (solid line) at $t_2 = 1.8$; $\Delta x = 0.01$. Unified coordinates, $h = 1$ (Lagrangian).

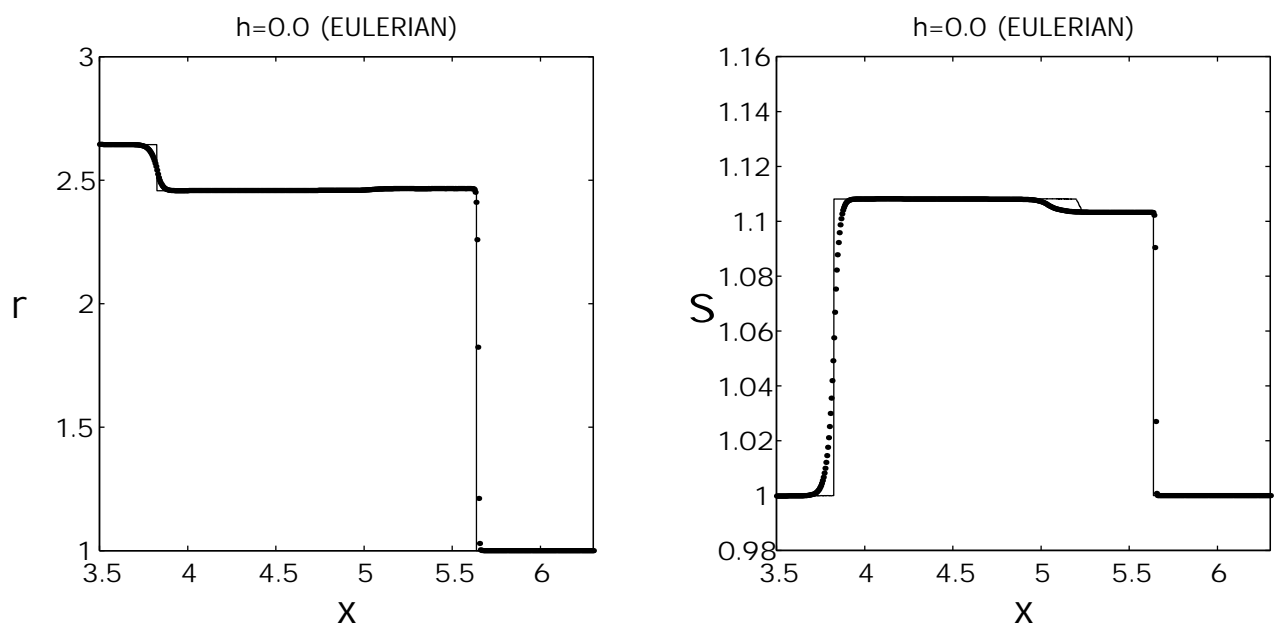


Figure 31: Computed (dots) density and entropy for the piston problem using Godunov-MUSCL scheme, compared with exact solution (solid line) at $t_3 = 3.0$; $\Delta x = 0.005$. Unified coordinates, $h = 0$ (Eulerian).

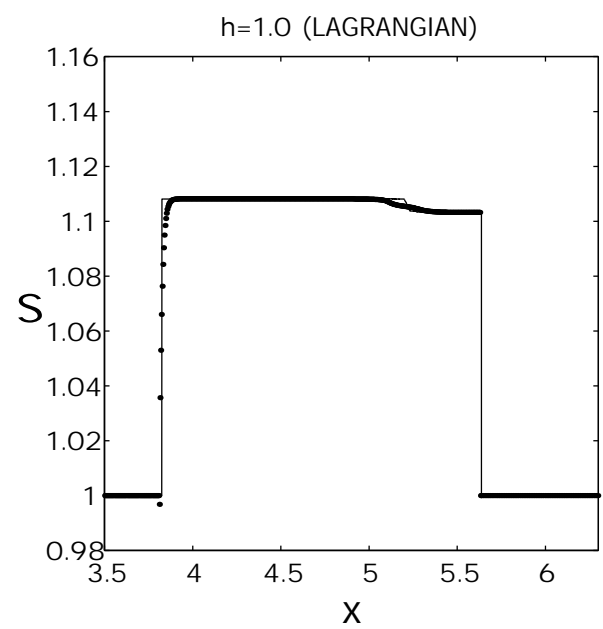
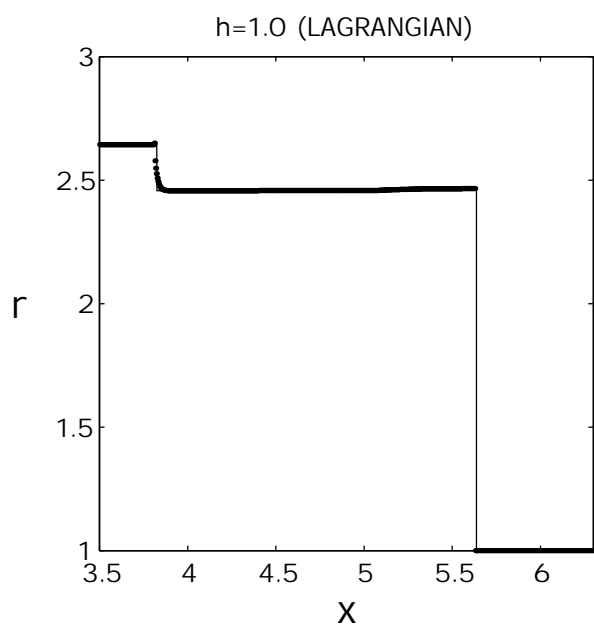


Figure 32: Computed (dots) density and entropy for the piston problem using shock-adaptive Godunov scheme, compared with exact solution (solid line) at $t_3 = 3.0$; $\Delta x = 0.01$. Unified coordinates, $h = 1$ (Lagrangian).

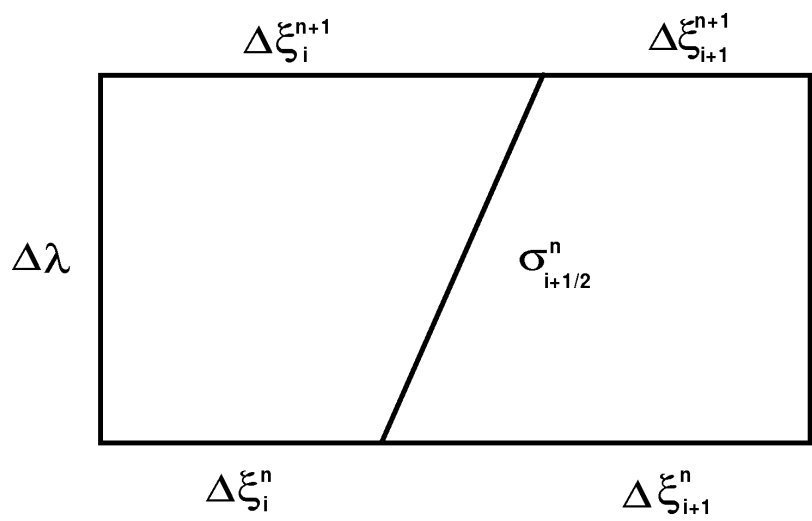


Figure 33: Computational cells i and $i + 1$ with partition in between having slope $\sigma_{i+1/2}^n$.